Improving GPR Signal Modelling for Efficient Characterization of Multi-layered Media

Subrata Maiti, Sarat Kumar Patra
Department of ECE
NIT, Rourkela
Odisha-769008, India
Email: smaiti@nitrkl.ac.in, skpatra@nitrkl.ac.in

Amitabha Bhattacharya
Department of E&ECE
IIT Kharagpur
West Bengal-721302, India
amitabha@ece.iitkgp.ernet.in

***Abstract*—We propose a plane wave model (PWM) which is derived based on analytical solution of a full wave model (FWM) applied to ground penetrating radar (GPR) signal propagation in layered media. The computation efficiency of PWM is enormous, and accuracy is comparable to FWMs. In this model, reflections from different interfaces and their higher order terms are expressed separately resulting in infinite number of terms for the forward model computation. The mathematical expression of PWM becomes complicated as the number of layers increases, and higher order reflections are considered for better accuracy of the model. It is observed that by applying suitable time window and limiting order of reflections based on GPR system dynamic range, the PWM expression can be simplified to a great extent. The effectiveness of the proposed method is verified by inverting synthetic data of a three layered (3L) media.**

***Index Terms*—Ground penetrating radar (GPR), Green's function, inverse modelling, SFCW radar, layered media**

I. Introduction

Quantitative reconstruction of sub-surface media by ground penetrating radar (GPR) technique finds many applications in the field of civil engineering, mining, geological survey, archeology, etc. [1]. The accuracy and speed of GPR detection strongly depend on the architecture of the GPR system. Monostatic off-ground GPR has the advantage of achieving high scanning speed with decreased penetration depth [2], [3]. The accuracy of GPR signal model and its computation efficiency have a great impact on the efficiency of a GPR system. Achieving both i.e. the accuracy and efficiency by effective modelling is a difficult task because of complex media property. Compared to the numerical methods [4], [5], analytical methods are time efficient and application specific. Among various analytical methods, full wave models (FWMs) [6–8] are very accurate methods for characterization of layered media. However, their computation efficiency is poor compared to the other simplified methods based on plane wave approximation. In [8], two plane wave models, i.e. PWM-1 and PWM-2 are proposed based on the analytical solution of an FWM. Laboratory testing on layered media and comparison analysis with synthetic data have demonstrated that, the PWMs are highly time efficient and as accurate as the FWMs [6], [8]. The PWMs express the Green's function by summation of reflections from different interfaces and their higher order terms. As the number of layers increases, the analytical expressions of PWMs become complicated with exponentially increasing number of terms to compute.

In this work, we have improved the PWMs for efficient characterization of multi-layered media. First, the PWMs are represented by a generalized formula. Then, the property of PWMs is exploited to reduce its computation complexity by using time domain Green's function scaled with a suitable time window. An improved method of layer stripping (LS) is realized with the help of PWM-2. The proposed LS can give apriori information about complete electrical parameters of layered media even in the presence of measurement and calibration errors. This, in turn helps to realize the complete inversion of the model by applying gradient method.

II. Proposed Method

The derivation of PWMs is elaborately discussed in [8]. Here we present a brief discussion on it. A generalized formula is presented to express the PWMs for multi-layered media with higher order reflections in Sec. II-A. Then a frequency-domain inversion (FDI) and a time-domain inversion (TDI) methods are presented in Sec. II-B to overcome the limitation of PWM-2. Finally, the LS technique is proposed in Sec. II-C for complete inversion of layered media electrical parameters.

A. Model Formulations

The stepped frequency continuous wave (SFCW) GPR system can be realized in the laboratory with a VNA, and a TEM horn antenna. The assumptions of monostatic and far-field GPR configuration are elaborately discussed in [2], [6]. In order to consider the effect due to the antenna, a linear transfer function model is used to represent the monostatic antenna and the media under test as shown in Fig. 1. Here $X(\omega)$ and $Y(\omega)$ are the transmit and receive signals at the VNA reference plane; $H_i(\omega)$ is the return loss of the antenna, $H_t(\omega)$ and $H_r(\omega)$ are the transmit and receive transfer functions of the antenna, and $H_f(\omega)$ represents the feedback loss transfer function. $G^{\uparrow}_{xx}(\omega)$ is the Green's function representing response due to the air-subsurface media. The VNA measured complex reflection coefficient $S_{11}(\omega)$ is expressed as following.

$$S_{11}(\omega) = \frac{Y(\omega)}{X(\omega)} = H_i(\omega) + \frac{H_t(\omega)\, G^{\uparrow}_{xx}(\omega) H_r(\omega)}{1 - H_f(\omega)\, G^{\uparrow}_{xx}(\omega)} \quad (1)$$

All these frequency dependent transfer functions can be extracted by a set of measurements by placing the antenna at different heights above a large size perfect electric conductor (PEC), and then solving a set of linear equations [9]. The

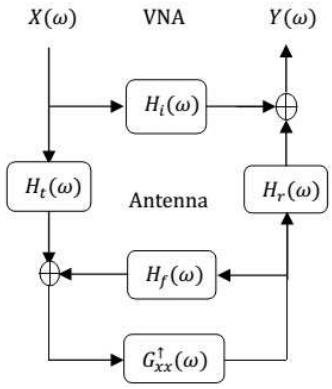

Fig. 1. Linear transfer functions representing the monostatic GPR system.

air-ground surface media is modeled as a 3-D multi-layered media consists of N horizontal layers separated by $N-1$ interfaces as illustrated in the Fig. 2. Any single n^{th} layer is homogeneous and is characterized by its complex permittivity $\epsilon_{e,n}\ \left(=\epsilon_n+\frac{\sigma_n}{i\omega}\right)$, permeability μ_n and thickness h_n. The assumption of planner media for the monostatic radar is logical as long as variation of media property is negligible with in the spatial and range resolution of the GPR system [2]. The frequency dependent electrical property of the materials is most accurately described by the Debye relation [10]. For a limited frequency band, the ϵ is assumed to be constant and σ is assumed to be a linear function of the frequency as following.

$$\sigma\left(f\right)=\sigma_c+\sigma_r\left(f-f_c\right) \tag{2}$$

where σ_c is the static conductivity (S/m) at center frequency f_c, and σ_r is the linear variation rate of it (S/m/GHz). For most of the materials $\mu_r=\mu_0$ i.e. the free space permeability.

The antenna is assumed to be a point source and receiver at its phase center, and it is located at the origin O of the coordinate system. The Green's function is defined as the ratio between the back scattered and the transmitted electric fields acting in the x-direction. By applying Huygen's field equivalence principle [11] ($pp.\ 575-581$), and solving 3-D Maxwell's equation for wave propagation, the Green's function due to the air-subsurface media is derived in spectral domain as following [8].

$$\tilde{G}_{xx}^{\uparrow}\left(k_\rho,\omega\right)=\left[R_n^{TE}-R_n^{TM}\right]e^{-2\Gamma_n h_n} \tag{3}$$

where R_n^{TE} and R_n^{TM} are, respectively, the transverse electric and the transverse magnetic global reflection coefficient accounting for all reflections from the multilayered interfaces [12] ($pp.\ 48-53$). $\Gamma_n\ \left(=\sqrt{k_\rho^2-k_n^2}\right)$ is the vertical wave number, k_n is the free space propagation constant of n^{th} layer defined as $k_n^2=-\zeta_n\eta_n$, $\zeta_n=i\omega\mu_n$, and $\eta_n=\sigma_n+i\omega\epsilon_n$. The spatial domain Green's function at the source point $((x,y,z)=0)$ is expressed as following.

$$G_{xx}^{\uparrow}(0,\omega)=\frac{1}{4\pi}\int_0^{+\infty}\tilde{G}_{xx}^{\uparrow}\left(k_\rho,\omega\right)k_\rho dk_\rho \tag{4}$$

Here, the variable k_ρ is a spectral domain parameter. The Green's function expression in Eq. 3 is similar to the Green's function expression in [6]. It is found that, they are highly correlated and differed by a constant factor [8]. These FWMs Green's functions take longer time for integration, causing GPR detection process to be slow. This problem is addressed

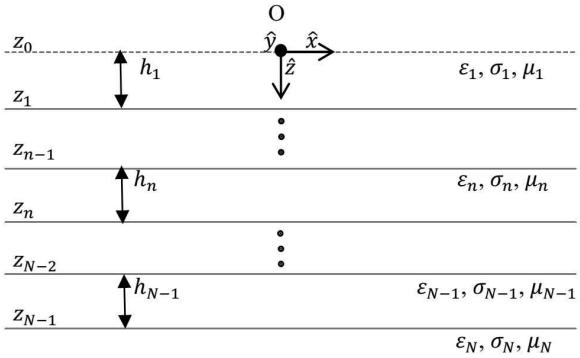

Fig. 2. N-layered medium with a point source at top.

by proposing PWMs [8] with PWM-2 being most accurate among them. They are derived based on the analytical solution of Eq. 3 and Eq. 4. In PWM-2, the 1^{st} order reflection from interface z_n is given by the following formula.

$$R_{n,n+1}^1=\left(\frac{\hat{r}_{n,n+1}^1}{2\pi i}\right)\left(\frac{1}{2\sum_{j=1}^n h_j/\gamma_j}+\frac{\left(\sum_{j=1}^n h_j/\gamma_j^3\right)}{4\left(\sum_{j=1}^n h_j/\gamma_j\right)^3}\right) \tag{5}$$

where

$$\left(\hat{r}_{n,n+1}^1\right)=r_{n.n+1}\prod_{j=1}^{n-1}\left(1-\left(r_{j,j+1}\right)^2\right)\prod_{j=1}^{n}exp(-2\gamma_j h_j) \tag{6}$$

$r_{j,j+1}$ is the reflection coefficient at j^{th} layer interface (z_j) for plane wave propagation as given below.

$$r_{j,j+1}=\frac{Z_{j+1}-Z_j}{Z_{j+1}+Z_j} \tag{7}$$

where $Z_j\left(=\sqrt{\frac{\zeta_j}{\eta_j}}\right)$ is the impedance of j^{th} layer media. The propagation parameter γ_j is given by

$$\gamma_j=\alpha_j+i\beta_j=\sqrt{\zeta_j\eta_j}=\sqrt{i\omega\mu_j(\sigma_j+i\omega\epsilon_j)}=ik_j \tag{8}$$

Let us modify the Eq. 5 in the following form.

$$R_{n,n+1}^1=\left(r_{n.n+1}\prod_{j=1}^{n-1}\left(1-\left(r_{j,j+1}\right)^2\right)\right)\frac{1}{2\pi i}$$
$$\left(\frac{1}{2\sum_{j=1}^n h_j/\gamma_j}+\frac{\left(\sum_{j=1}^n h_j/\gamma_j^3\right)}{4\left(\sum_{j=1}^n h_j/\gamma_j\right)^3}\right)\left(\prod_{j=1}^{n}exp(-2\gamma_j h_j)\right)$$
$$=L_{R_n}^1 L_{S_n}^1 exp\left(\sum_{j=1}^{n}-2\gamma_j h_j\right) \tag{9}$$

where $L_{R_n}^1=r_{n.n+1}\prod_{j=1}^{n-1}\left(1-\left(r_{j,j+1}\right)^2\right)$ and $L_{S_n}^1=\frac{1}{2\pi i}\left(\frac{1}{2\sum_{j=1}^n h_j/\gamma_j}+\frac{\left(\sum_{j=1}^n h_j/\gamma_j^3\right)}{4\left(\sum_{j=1}^n h_j/\gamma_j\right)^3}\right)$. Here $L_{R_n}^1$ represents

the losses due to reflections and refractions at different interfaces and $L^1_{S_n}$ represents the spherical spreading loss for travelling the path $\sum_{j=1}^{n} 2h_j$. A generalized formula can be written as below to represent the reflection coefficients due to m^{th} order reflections from interface z_n.

$$R^m_{n,n+1} = \sum_{k=1}^{P^m_n} L^{m,k}_{R_n} L^{m,k}_{S_n} exp\left(\sum_{j=1}^{n} -2\gamma_j a_j h_j\right) \tag{10}$$

where a_j are $+$ve integers having values more than one, and are related by the following inequality.

$$n + m - 1 \leq \sum_{j=1}^{n} a_j \leq (n-1)\, m + 1 \tag{11}$$

P^m_n is the total number of possible combinations by which the inequality (Eq. 11) is satisfied. $L^{m,k}_{R_n}$ is the losses due to reflections and refraction in multiple interfaces and $L^{m,k}_{S_n}$ is the spreading loss for the k^{th} path. The $L^{m,k}_{S_n}$ is simple to find by the following expression.

$$L^{m,k}_{S_n} = \frac{1}{2\pi i}\left(\frac{1}{2\sum_{j=1}^{n} a_j h_j/\gamma_j} + \frac{\left(\sum_{j=1}^{n} a_j h_j/\gamma_j^3\right)}{4\left(\sum_{j=1}^{n} a_j h_j/\gamma_j\right)^3}\right) \tag{12}$$

The $L^{m,k}_{R_n}$ depends on the path followed by the signal. It is easy to calculate them for a limited number of layers. As an example, the $L^{m,k}_{R_n}$ for m^{th} order reflection from z_2 is expressed as

$$L^{m,1}_{R_2} = \left[r_{2,3}\left(1 - r^2_{1,2}\right)\left(r_{2,1} r_{2,3}\right)^{(m-1)}\right]. \tag{13}$$

Here P^m_2 is 1, as there is only one way the higher order reflections are possible. The overall PWM-2 Green's function for maximum order N_o from all the interfaces (z_1 to z_{N-1}) can be expressed as following.

$$G^{\uparrow \mathrm{PWM}}_{xx}(\omega) = \sum_{k=1}^{N_o}\sum_{j=1}^{N-1} {R^k}_{j,j+1} \tag{14}$$

By neglecting h^2 variation from ${R^k}_{j,j+1}$, the Eq. 14 represents the PWM-1 Green's function. The PWMs have been analyzed rigorously and compared with the FWMs for a three-layered media in terms of correlation coefficients and average RMS differences [8]. It is found that the PWM-2 is highly correlated with FWMs as we consider for the higher order (N_o) terms. However, as we consider for higher order reflections from multi-layer interfaces, computation of refection and transmission loss ($L^{m,k}_{R_n}$) becomes difficult task with number of possible paths (P^m_n) increasing exponentially. The accuracy of PWMs degrades, if higher order terms are neglected for computing the layered media Green's function. There can be a limit for the N_o value based on GPR system dynamic range requirements, instrument capability, prevailing noise, measurement error, and external interferences. In the cases, where either $L^{m,k}_{S_n}$ or $L^{m,k}_{R_n}$ of the layers are high, the N_o can be taken as small number. It would be possible to derive PWM-2 as accurate as FWMs for finite number (N) of layers. In subsequent section, we will explore to reduce the complexity of PWMs.

B. Model Inversion Approaches

For the SFCW monostatic GPR, the uncertainty in the inverted model parameters is largely originated due to the calibration error, height measurement error, instrument instability with respect to time and environment conditions, noise, interference, etc. [9], [13]. It is reported that the calibration error contributes to error in Green's function extraction and limit the usable band-width of the SFCW GPR system. The antenna height measurement error causes tremendous uncertainties on the reconstruction of layered media parameters. While working with inversion with synthetic data, it is very important to analyze the performance of the proposed model in the presence of various sources of errors and noise.

For inverting the PWMs, we define two kinds of objective function i.e. one in the frequency domain and other in the time domain. For frequency domain inversion (FDI), the objective function $\Phi(b)$ is defined in the least square sense as following.

$$\Phi\left(b\right) = \left|G^{\uparrow *}_{xx}\left(\omega\right) - G^{\uparrow}_{xx}(\omega, b)\right|^T \left|G^{\uparrow *}_{xx}\left(\omega\right) - G^{\uparrow}_{xx}(\omega, b)\right| \tag{15}$$

where $G^{\uparrow *}_{xx}\left(\omega\right)$ and $G^{\uparrow}_{xx}(\omega, b)$ are the vector containing, respectively, measured and simulated Green's function of the multilayered media. The parameters vector b (consists of $\mu_n, \epsilon_n, \sigma_n, h_n$) needs to be reconstructed by minimizing the objective function $\Phi\left(b\right)$ in Eq. (15). It can be observed that, every reflections are denoted by separate terms in PWMs (Eq. 14). Therefore, we can limit the number of terms based on the required observation time window. This time window can be defined, either starting from 0 to the time instant of 1^{st} order reflection from the last layer of our interest, or it can be focussed on a particular layer of our interest. In second case, the previous layers parameters must be known. Therefore, we propose the objective function for the time domain inversion (TDI) based on cross correlation coefficient (CCC) between the measured and simulated models as following.

$$\Phi^t\left(b\right) = \frac{1}{CCC\left(G^{\uparrow *}_{xx}(t), G^{\uparrow}_{xx}(t, b)\right)} \tag{16}$$

where $G^{\uparrow *}_{xx}(t)$ and $G^{\uparrow}_{xx}(t, b)$ are the measured and simulated Green's function in time domain, and limited by an observation time window. These objective functions are highly non-linear and have multiple minima. We use a gradient based approach for inverting the model. Since, gradient based technique can't converege unless the starting parameters values are in global basin, a layer stripping (LS) technique is utilized to get preliminary information on electrical parameters of the media.

C. Layer Stripping (LS) Method

LS is used for many years for approximate and fast calculation of electrical parameters of the layered media [3], [14]. In this method, GPR processing is done in the time domain for reconstruction of each layer in step by step starting from the top layer. In most of the cases, there are common assumptions like plane wave propagation and neglecting the presence of multiple reflections. In [14], authors have tried to improve this method by applying dispersion correction, energy-based detection method, super resolution technique, etc. However, this method is based on the assumption of loss less media. The main drawbacks of the existing techniques are the accumulation of error due to recursive formulations.

The proposed method is based on common LS technique and the TDI focusing on a limited number of reflection to reconstruct the property of one layer at a time. The method is named as layer stripping by inversion method (LSIM). The process starts with time domain processing of the measured Green's function $G_{xx}^{\uparrow *}(t)$. First, the timing information (t_i) and amplitude values for all the 1^{st} order significant reflections (P_i) are evaluated. An appropriate synthetic pulse needs to be used for reducing range side lobes, and an accurate algorithm has to be applied to extract the timing and amplitude information of the reflected pulses. For any N^{th} layered media, 1^{st} layer is the air media. It's thickness h_1 i.e. height of the antenna can be easily evaluated by the relation $h_1 = \frac{(c \times t_1)}{2}$. Here c is the velocity of EM wave at free space. Then following steps need to be applied for realizing the LSIM.

Step 1: 1^{st} layer property is known i.e. h_1, ϵ_{r_1}, σ_{c_1} and σ_{r_1} are known. For air media $\epsilon_{r_1} = 1$, and $\sigma_{c_1} = \sigma_{r_1} = 0$. Then generate a Green's function for the media having 1^{st} layer property as ϵ_{r_1}, σ_{c_1}, σ_{r_1}, and h_1, and a PEC at layer 2. Find the reflection P_1^{pec} from the interface z_1 by time-domain processing. Now compare the P_1 with P_1^{pec} and use the following approximate formula to find ϵ_{r_2}.

$$-\frac{P_1}{P_1^{pec}} = r_{1,2} = \frac{\sqrt{\epsilon_{r_1}} - \sqrt{\epsilon_{r_2}}}{\sqrt{\epsilon_{r_1}} + \sqrt{\epsilon_{r_2}}} \tag{17}$$

Step 2: Apply the GPR inversion with a time window focusing on P_1 to invert the parameters vector b consists of seven parameters i.e. ϵ_{r_1}, σ_{c_1}, σ_{r_1}, h_1, ϵ_{r_2}, σ_{c_2}, and σ_{r_2}. Initial values for σ_{c_2}, and σ_{r_2} can be chosen either arbitrarily or equate to the values of σ_{c_1}, and σ_{r_1} respectively.

Step 3: Update the ϵ_{r_2} based on the inversion result obtained in Step 2. Find the thickness h_2 by the following relation.

$$h_2 = \frac{c \times (t_2 - t_1)}{2\beta_2/\beta_0} \approx \frac{c \times (t_2 - t_1)}{2\sqrt{\epsilon_2}} \tag{18}$$

Now repeat the step 1 to 3 for next layer and repeat them till all the layers are evaluated. Here step 2 helps to stop the error propagation by improving the accuracy of the parameters by using TDI based on accurate model PWM-2.

The ability to find accurate values for current layer parameters ϵ_{r_n}, σ_{c_n}, σ_{r_n}, h_n and next layer parameters $\epsilon_{r_{n+1}}$, $\sigma_{c_{n+1}}$, and $\sigma_{r_{n+1}}$ depends on the sensitivity of time domain objective function ($\Phi^t(b)$) on these parameters. We have done a response surface analysis to find sensitivity of $\Phi^t(b)$ for a 3L media with respect to the variation of parameters ϵ_{r_2}, σ_{c_2}, h_2, ϵ_{r_3}, and σ_{c_3}. Here $\Phi^t(b)$ is bounded by a time window focusing on 1^{st} order reflection from interface z_2. It revealed that the $\Phi^t(b)$ is less sensitive to σ in the lower range of parameter values. Better quality of signal is required to resolve conductivities accurately. The $\Phi^t(b)$ being more sensitive to ϵ_r and h, they can be retrieved accurately by the TDI method. For good quality signal, the complexity of LSIM can be reduced by reducing number of optimization variables to 5 (σ_{c_1}, σ_{r_1}, ϵ_{r_2}, σ_{c_2}, and σ_{r_2}) or just 3 (ϵ_{r_2}, σ_{c_2}, and σ_{r_2}) for faster implementation of the process. To improve the accuracy of inversion in the Step 3, $\Phi^t(b)$ can be defined over a time-window focusing on two consecutive reflections i.e. one from current interface and other from the previous interface. It is also obsreved that, application of a global optimization technique further improves the accuracy of parameters estimation.

III. Results and Discussion

GPR detection process starts with GPR calibration process, followed by measurement on the media under test, and finally, software simulation to invert the model to retrieve the media parameters. In this work, we present our analysis of a three-layered (3L) media with synthetic data generated by the FWM proposed in Sec II-A. A 3L media is created by placing open half space on top and a known media at the bottom. This media is equivalent to a 5L media based on Fig. 2. We analyze the effects of two major sources of errors i.e. the effect of calibration height measurement error, and the effect of height measurement error on GPR detection. To add calibration height measurement error, the height error of uniform variance (σ_h) varying from 0 to 1 mm is added by following the process explained in [9]. An error of ± 0.5 mm is added with the actual height of the antenna to simulate the effect of the antenna height measurement error on the GPR detection. For comparing the performances of FDI and TDI, we take two models of 3L media i.e. 3L-M1 (Sec. III-A), and 3L-M2 (Sec. III-B) with a thin layer placed at layer 3. For both FDI and TDI, we choose actual media parameters as the initial parameters vector for gradient based optimization. In Sec. III-C, the complete model inversion approach with the help of LSIM and gradient method is presented. In this case, there is no previous knowledge on the initial model configuration or model parameters. The SFCW GPR system parameters are specified by the requirement of range, resolution, sensitivity, scanning speed, level of clutters etc. For synthetic model verification, we select a frequency band of 1 GHz to 3 GHz with frequency spacing of 40 MHz based on our model configuration requirements. For converting to time domain, we perform 4096 points IFFT, which can give height measurement accuracy of 0.3 mm in ideal case.

A. Inversion of Synthetic 3L Media

A 3L model (3L-M1) is taken with layer parameters as $\epsilon_r = [1, 2.4, 9, 25, 6]$, $h = [35, 20, 10, 10, \infty]$ cm, $\sigma_c = [0, 15, 18, 20, 20]$ mS/m, and $\sigma_r = [0, 10, 10, 10, 0]$ mS/m/GHz. For FDI, the PWM-2 is computed with maximum order N_o as 4. By setting $N_o = 4$, the ratio between the most significant reflection and least significant higher order reflection is 72 dB at center frequency $f_c = 2$ GHz. In this case, more than 50 reflection terms are required to be included for computing PWM-2 Green's function even after neglecting many insignificant 4^{th} order terms originated from z_4. For TDI, only the necessary terms are computed which are placed between 1^{st} order reflections from interfaces z_1 and z_4. In this case, we require to compute just 10 terms with maximum 3^{rd} order terms from z_2, 2^{nd} order terms from z_3 and 1^{st} order term from z_4. Then, the synthetic Green's functions $G_{xx}^{\uparrow}(\omega)$ are generated after adding calibration height measurement errors. Then TDI and FDI are carried out with antenna height measurement errors of 0 and ± 0.5 mm. The results of inversion are presented in the Table I. It can be observed that, the TDI is able to invert the model parameters with almost same correlation coefficients as FDI. The fluctuation of inverted parameters is observed for both the inversion methods.

TABLE I. INVERTED PARAMETERS OF 3L-M1 FOR TDI AND FDI

σ_h (mm)	Δh (mm)	ϵ_{r_2}	σ_{c_2} (S/m)	σ_{r_2} (S/m/GHz)	h_2 (cm)	ϵ_{r_3}	σ_{c_3} (S/m)	σ_{r_3} (S/m/GHz)	h_3 (cm)	ϵ_{r_4}	σ_{c_4} (S/m)	σ_{r_4} (S/m/GHz)	h_4 (cm)	t (s)	$\%CCC$
Time Domain Inversion (TDI) Results															
0	0	2.40	15.00	10.00	20.00	9.00	18.00	10.00	10.00	25.00	20.00	10.00	10.00	1.56	99.9999
0	0.5	2.86	11.74	11.74	18.28	9.28	19.23	10.21	9.86	22.46	21.01	10.05	10.05	5.55	99.9818
0	-0.5	2.05	17.71	8.74	21.68	9.30	15.60	9.78	9.83	28.96	19.23	9.99	9.29	6.46	99.9958
1	0	2.08	17.56	9.66	21.48	9.44	15.84	9.81	9.76	28.84	18.35	9.91	9.31	6.56	99.9581
1	0.5	2.45	14.79	11.00	19.79	9.17	18.00	10.07	9.91	24.94	19.97	9.99	10.01	4.25	99.9696
1	-0.5	1.92	19.04	9.21	22.40	9.98	13.67	9.66	9.48	32.05	17.42	9.91	8.78	7.28	99.9339
Frequency Domain Inversion (FDI) Results															
0	0	2.40	14.89	10.02	20.00	8.94	18.59	9.95	10.04	24.91	19.24	9.56	10.02	7.55	99.9999
0	0.5	2.41	11.96	9.70	19.91	7.52	27.97	11.50	10.95	22.15	4.30	1.36	10.62	22.01	99.9584
0	-0.5	2.39	17.90	10.32	20.09	11.14	19.82	8.99	8.99	35.90	40.60	17.03	8.34	22.62	99.9596
1	0	2.45	16.21	9.93	19.83	9.83	14.40	15.00	9.58	25.80	25.07	3.71	9.83	15.61	99.8855
1	0.5	2.46	13.07	9.51	19.73	8.07	26.19	15.39	10.58	22.06	3.73	0.00	10.63	15.15	99.9494
1	-0.5	2.43	16.86	10.15	19.94	10.07	13.01	13.55	9.46	26.63	24.35	8.49	9.68	12.41	99.6962

TABLE II. INVERTED PARAMETERS OF 3L-M2 FOR TDI AND FDI

σ_h (mm)	Δh (mm)	ϵ_{r_2}	σ_{c_2} (S/m)	σ_{r_2} (S/m/GHz)	h_2 (cm)	ϵ_{r_3}	σ_{c_3} (S/m)	σ_{r_3} (S/m/GHz)	h_3 (cm)	ϵ_{r_4}	σ_{c_4} (S/m)	σ_{r_4} (S/m/GHz)	h_4 (cm)	t (s)	$\%CCC$
Time Domain Inversion (TDI) Results															
0	0	2.40	15.00	10.00	20.00	9.00	18.00	10.00	10.00	25.00	20.00	10.00	2.00	1.04	99.9999
0	0.5	2.88	11.61	11.61	18.22	9.42	28.82	12.81	9.78	26.54	21.71	10.46	1.94	11.72	99.9925
0	-0.5	1.99	16.43	8.06	22.02	7.95	11.93	9.34	10.63	21.85	19.14	9.85	2.14	7.31	99.9973
1	0	2.01	16.21	9.48	21.85	7.99	12.28	4.22	10.60	21.69	17.99	9.06	2.15	8.91	99.9741
1	0.5	2.48	14.69	10.93	19.63	9.31	18.70	9.30	9.83	25.57	19.85	9.88	1.98	6.93	99.9803
1	-0.5	1.92	18.70	9.88	22.40	9.63	0.85	0.00	9.64	26.22	15.87	8.35	1.96	13.49	99.9554
Frequency Domain Inversion (FDI) Results															
0	0	2.40	14.20	10.40	20.00	8.54	19.66	8.38	10.27	23.36	24.92	0.00	2.07	8.66	99.9990
0	0.5	2.40	13.77	10.05	19.94	8.39	20.86	9.72	10.36	23.00	25.71	0.00	2.09	9.63	99.9625
0	-0.5	2.39	14.54	10.68	20.08	8.64	18.49	7.15	10.21	23.62	24.13	0.00	2.06	9.29	99.9496
1	0	2.45	14.87	10.60	19.83	8.93	21.62	10.38	10.05	24.21	11.51	0.00	2.02	8.55	99.9054
1	0.5	2.46	14.47	10.22	19.75	8.80	22.92	11.95	10.11	23.88	12.13	0.00	2.04	8.75	99.9565
1	-0.5	2.43	15.17	10.88	19.93	9.02	20.34	8.95	10.00	24.43	10.91	0.00	2.01	8.43	99.7700

B. Inversion of Synthetic 3L Media with Thin Layer

The same experiment is repeated for the second model i.e. 3L-M2 with a thin layered media placed at third layer with a PEC at the bottom. The layer parameters are $\epsilon_r = [1, 2.4, 9, 25, 6]$, $h = [35, 20, 10, 2, \infty]$ cm, $\sigma_c = \left[0, 15, 18, 20, 6 \times 10^9\right]$ mS/m, and $\sigma_r = [0, 10, 10, 10, 0]$ mS/m/GHz. It can be observed that, the minimum requirement of band-width $\times$ time-resolution is 1.33 for the GPR System. The thin layer placed at the bottom most layer above a PEC is the most difficult case for the PWM-2 inversion. The higher order reflections from z_4 overlap with each other in time domain, and they don't diminish early because of PEC reflections. For FDI, the N_o is taken as 4 for reflections from z_2, and z_3, and 10 for reflections from z_4. However, only the significant reflections are computed based on the attenuation analysis at the center frequency. Even after increasing the value of N_o, the ratio between the most significant reflection and the least significant higher order reflection is observed as 53 dB. The model computation is much easier for TDI with few terms required to compute the model. However, till 5^{th} order reflections are considered from interface z_4 as some of them overlap with the 1^{st} order reflection from z_4. The results of models inversion are presented in Table II. It can be observed that the TDI leads to better cross correlation coefficients between the inverted and the input models compared to the FDI. The TDI takes much less time compared to the FDI for the error-free synthetic data. However, the timing required for both the inversion methods are similar while inverting error data. This observation can be explained by the fact that, the inversion time depends on the forward model computation speed, the convergence property of the model, the error in the input data, etc.

C. Complete Inversion of Model

The 3L-M1 is selected for simulation analysis of complete inversion with the help of LSIM and gradient method. In the first case, we consider the error-free synthetic data generated by the FWM as the input data. In the second case, the synthetic data is modified with the calibration height measurement error of $\sigma_h = 1$ mm and then LSIM and TDI are carried out after introducing antenna height measurement error as 0.5 mm. The results are presented in Table III. The LSIM outputs for the different layers are presented in the 1^{st} three rows of the table. The final inversion results are presented in the 4^{th} row. It can be observed that, the inversion can't yield the correct parameters values, even in the case of error free data. This error is mostly due to the limitation of gradient method of optimization, which can't find the global minima in presence of local minima. Secondly, there is a small difference between the PWM-2 and the FWM Green's functions. For the second case of inversion, it can be observed that, the third layer parameters are changed significantly. This happens due to the degraded signal to noise ratio for the signals originated from the interfaces z_3 and z_4 compared to the other interfaces. Fig. 3 presents the plots for the time domain Green's functions ($G^{\uparrow}_{xx}(t)$) for the inverted models and the input models defined over the time window spanning between the 1^{st} order reflections from interfaces z_1 and z_4.

Discussion: The inversion results with the proposed methods, i.e., FDI and TDI demonstrate that both are useful methods to realize PWM-2 inversion. The TDI has the advantage of ease of model computation for multi-layered media with reduced number of terms. The TDI approach indeed helps to reduce the complexity of PWMs and thereby makes them suitable for multi-layered media applications. The complete

TABLE III. INVERTED PARAMETERS OF 3L-M1 WITH THE HELP OF LSIM AND TDI

σ_h (mm)	Δh (mm)	ϵ_{r_2}	σ_{c_2} (S/m)	σ_{r_2} (S/m/GHz)	h_2 (cm)	ϵ_{r_3}	σ_{c_3} (S/m)	σ_{r_3} (S/m/GHz)	h_3 (cm)	ϵ_{r_4}	σ_{c_4} (S/m)	σ_{r_4} (S/m/GHz)	h_4 (cm)	t (s)	$\%CCC$
Results of LSIM and complete inversion for error free data as input															
0	0	2.40	15.00	10.00											
		2.41	15.01	10.00	19.97	9.05	15.00	10.00							
						9.21	15.01	10.06	9.88	24.92	15.00	10.00		3.84	
		2.21	15.02	9.16	20.84	8.71	15.33	9.97	10.06	24.46	15.34	9.97	10.11	7.03	99.9686
Results of LSIM and complete inversion for error data as input															
1	0.5	3.04	13.91	1.00											
		2.95	12.15	11.07	18.02	9.50	13.93	0.99							
						8.79	14.43	9.07	10.13	19.86	13.93	0.77		7.13	
		2.65	10.89	10.89	19.01	8.05	15.20	8.86	10.58	18.94	14.79	2.50	11.49	12.54	99.8940

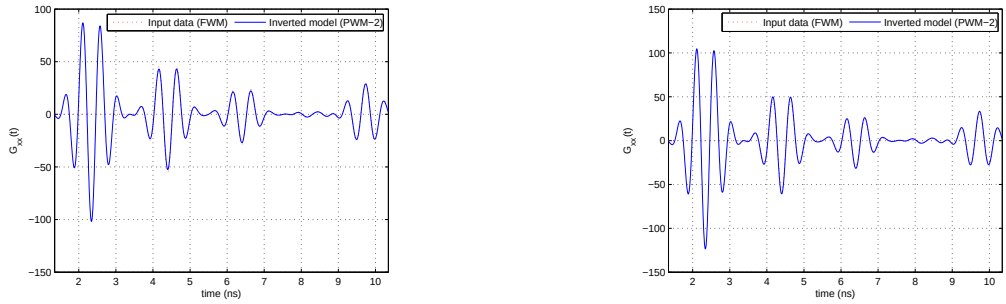

(a) (b)

Fig. 3. Compare input and inverted Green's functions in time domain for (a) error free data, and (b) data with error.

inversion approach with the help of LSIM and gradient method is promising. However, this approach needs to be validated by practical measurements. Based on the results of synthetic data, it can be said that, accurate antenna height measurements during GPR calibration and detection are very important for reducing uncertainties of the inverted media parameters.

IV. CONCLUSION

In this work, we have improved the model PWM-2 to make it more effective for reconstructing multi-layered media. The complexity of PWM-2 can be greatly reduced with the help of TDI approach for inverting multi-layered media. The effectiveness of both the inversion approaches i.e. TDI and FDI is demonstrated by applying them to two different model configurations of three layered media. They are found to be effective in the presence of calibration error, and height measurement error during GPR detection. The inversion approach with the help of LSIM and gradient method can be very effective to detect unknown layered media parameters. Experiments with synthetic three layered data demonstrate the capability. This integrated approach of inverse modelling can be a valued alternative for quantitative reconstruction of multi-layered media. The future work will focus on more rigorous analysis on the FDI, TDI, and LSIM techniques to verify their performances in the noisy practical scenarios.

REFERENCES

[1] D. J. Daniels, *Ground penetrating radar*. The Institution of Engineering and Technology, London,UK, 2007.

[2] G. G. Gentili and U. Spagnolini, "Electromagnetic inversion in monostatic ground penetrating radar: Tem horn calibration and application," *Geoscience and Remote Sensing, IEEE Transactions on*, vol. 38, no. 4, pp. 1936–1946, 2000.

[3] A. Loizos and C. Plati, "Accuracy of ground penetrating radar horn-antenna technique for sensing pavement subsurface," *Sensors Journal, IEEE*, vol. 7, no. 5, pp. 842–850, 2007.

[4] K. Belli, C. M. Rappaport, H. Zhan, and S. Wadia-Fascetti, "Effectiveness of 2-d and 2.5-d fdtd ground-penetrating radar modeling for bridge-deck deterioration evaluated by 3-d fdtd," *Geoscience and Remote Sensing, IEEE Transactions on*, vol. 47, no. 11, pp. 3656–3663, 2009.

[5] C. Warren and A. Giannopoulos, "Creating finite-difference time-domain models of commercial ground-penetrating radar antennas using taguchis optimization method," *Geophysics*, vol. 76, no. 2, pp. G37–G47, 2011.

[6] S. Lambot, E. C. Slob, I. van den Bosch, B. Stockbroeckx, and M. Vanclooster, "Modeling of ground-penetrating radar for accurate characterization of subsurface electric properties," *Geoscience and Remote Sensing, IEEE Transactions on*, vol. 42, no. 11, pp. 2555–2568, 2004.

[7] A. Kalogeropoulos, J. Van Der Kruk, J. Hugenschmidt, J. Bikowski, and E. Brühwiler, "Full-waveform gpr inversion to assess chloride gradients in concrete," *Ndt & E International*, vol. 57, pp. 74–84, 2013.

[8] S. Maiti, S. K. Patra, and A. Bhattacharya, "Gpr modeling for rapid characterization of layered media," *Progress In Electromagnetics Research B*, vol. 63, pp. 217–232, 2015.

[9] M. R. M. Ardekani and S. Lambot, "Full-wave calibration of time- and frequency-domain ground-penetrating radar in far-field conditions," *Geoscience and Remote Sensing, IEEE Transactions on*, vol. 52, no. 1, pp. 664–678, 2014.

[10] P. J. W. Debye, *Polar molecules*. Chemical Catalog Company, Incorporated, 1929.

[11] C. A. Balanis, *Antenna theory: analysis and design*. John Wiley & Sons, 2001.

[12] W. C. Chew, *Waves and fields in inhomogeneous media*. IEEE press New York, 1995.

[13] C. Patriarca, M. Miorali, E. Slob, and S. Lambot, "Uncertainty quantification in off-ground monostatic ground penetrating radar," *Antennas and Propagation, IEEE Transactions on*, vol. 61, no. 6, pp. 3334–3344, 2013.

[14] S. Caorsi and M. Stasolla, "A layer stripping approach for em reconstruction of stratified media," *Geoscience and Remote Sensing, IEEE Transactions on*, vol. 52, no. 9, pp. 5855–5869, 2014.